Preprints, 10th IFAC International Symposium on
Advances in Automotive Control
Columbus, Ohio, USA, August 28-30, 2022

Maximizing Work Extraction Efficiency of a Hybrid Opposed Piston Engine Through Iterative Trajectory Optimization ⋆

Joseph A. Drallmeier * **Charles E. Solbrig** *
Robert J. Middleton * **Jason B. Siegel** *
Anna G. Stefanopoulou *

* *Powertrain Control Lab, University of Michigan, Ann Arbor, MI, 48109 USA. (e-mail: drallmei, csolbrig, rjmidd, siegeljb, annastef@umich.edu).*

Abstract: This paper presents the real-time optimization of the crankshaft motion in a hybridized opposed piston (OP) engine using an iterative learning-based trajectory optimization scheme. The powertrain is oriented in a series hybrid design with each crankshaft directly coupled to electric motors, eliminating the conventional geartrain linking the two crankshafts along with the associated friction and weight. In this way, the electric motors can directly extract the work generated by the engine and regulate the crankshaft dynamics, introducing the capability to dynamically vary compression ratio, combustion volume, and scavenging dynamics on an inter-cycle basis. This control freedom increases the system's maximum potential efficiency, yet requires highly optimized intra-cycle crankshaft motion profiles to realize the improved work extraction efficiency of the dual motor-controlled OP engine. Leveraging the repetitive nature of the internal combustion engine, an iterative trajectory optimization (ITO) algorithm is used to define the optimal crankshaft motion profile in real-time for steady state operation. We demonstrate experimentally the rapid convergence and near optimal crankshaft motion profiles for the ITO strategy as well as its proficiency under both motored and fired cycle operation.

Keywords: Iterative Learning Control, Real-time Control, Convex Optimization, Trajectory and Path Planning, Parametric Optimization

1. INTRODUCTION

Hybrid electric powertrains improve vehicle efficiency through the flexibility provided by multiple onboard energy sources (Enang and Bannister (2017)). Power supplied from a secondary source enables more efficient operation with a downsized internal combustion engine. However, the decreased cylinder volume of smaller engines increases heat transfer and yields lower peak efficiencies for the same mean effective pressure (Payri et al. (2014)). Therefore, the opposed piston (OP) engine has been proposed as an alternative internal combustion (IC) engine design to maximize the potential efficiency of hybrid powertrains. (Young et al. (2021); Serrano et al. (2021); Drallmeier et al. (2021b)). Along with several thermodynamic benefits (Herold et al. (2011); Willcox et al. (2012); Pirault (2010)), the OP engine is inherently balanced in nature due to the two crankshafts operating opposite each other, allowing for downsizing though reduction in cylinder count rather than individual cylinder volume. This lends itself well to lower power, downsized, range extender or hybrid powertrain applications, without incurring the increased heat transfer losses of a conventional, four stroke internal combustion engine.

In an OP engine, two pistons face each other in a single cylinder, combining the stroke of both pistons while eliminating the cylinder head of a conventional IC engine. The OP engine operates on a uniflow scavenged two stroke cycle where the pistons actuate the intake and exhaust ports as shown in Fig. 1. A geartrain conventionally links the two crankshafts, coupling the motion of the pistons and ensuring a fixed exhaust crankshaft lead (ECL) which defines the relative phasing of the two crankshafts. Previous work by the authors highlight the potential for a dual motor-controlled OP engine (Drallmeier et al. (2021b)), wherein electric motors are coupled directly to each crankshaft. Not only does this configuration eliminate geartrain friction losses, but the electric motors can regulate the angular velocity of the crankshafts. With independent control of the piston trajectories and ECL, the capability to vary compression ratio, combustion volume, and scavenging dynamics is introduced on an inter-cycle basis. As shown in work from Young et al. (2021) as well as Naik et al. (2013), the optimal ECL for an OP engine varies depending the operational setpoint.

However, the dual-motor system efficiency is highly dependent on the operation and required control torque from the electric motors. Any gains in efficiency from removing the geartrain can be lost to poor motor performance. Results from Drallmeier et al. (2021b) show a near constant motor torque profile maximizes the work extraction efficiency of

⋆ This work was supported by the Automotive Research Center, U.S. Army DEVCOM GVSC. DISTRIBUTION A. Approved for public release; distribution unlimited. OPSEC # 6585

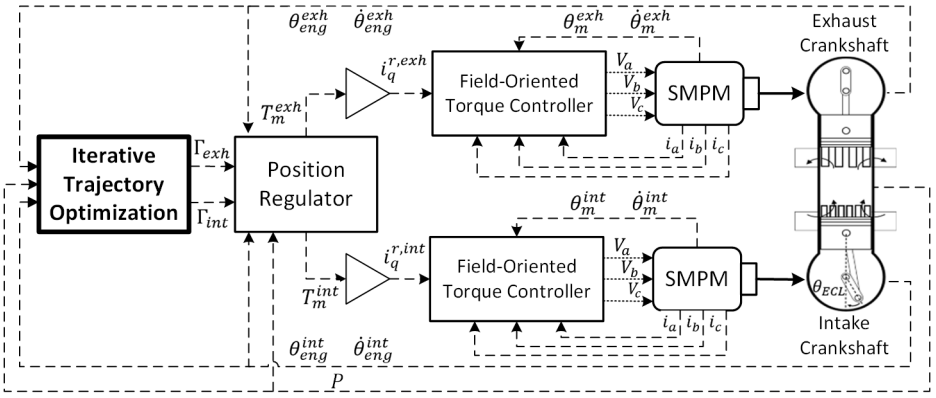

Fig. 1. Control architecture of the hybridized OP engine. Solid lines represent mechanical connections, dotted lines represent electrical connections, and dashed lines represent control or measurement signals. The trajectory optimization algorithm provides the basis parameters Γ defining the tracking reference to the lower level controls.

this system. Yet, the necessity to maintain the relative positioning between the two pistons requires control over the instantaneous crankshaft position and prohibits the use of constant intra-cycle torque control to maintain the desired engine speed. The challenge then is not in controlling the crankshaft to a desired position trajectory. Rather, it is defining the optimal position and velocity trajectory to control to. The system has shown significant sensitivity to model uncertainty, limiting the effectiveness of offline optimization (Drallmeier et al. (2021a)). The repetitive motion of the reciprocating IC engine can be leveraged to implement a learning-based scheme for iterative trajectory optimization (ITO) presented by the authors in Drallmeier et al. (2022). In this way, the information rich signals from the previous engine cycle can be used to improve the tracking reference of the next cycle based on the performance criteria. Further, the use of the previous cycle data reduces the reliance of the optimization process on the fidelity of the system model while still maintaining the required constraint on the relative phasing of the two crankshafts.

In the following sections, the experimental test setup and control system along with the relevant system dynamics are described. Then, the trajectory optimization problem is introduced by first briefly describing the ITO process followed by the parameterized trajectory variables and associated cost function for the hybrid OP powertrain. Finally, results showing the effectiveness of the learning scheme during motored conditions as well as for fired conditions are presented. Not only does the ITO method reduce calibration time, eliminating the need for a table of motion profiles to be calculated offline for different speed and load setpoints, but it also enables downsizing of the electric motors used for controlling the crankshaft motion, reducing cost and weight while increasing motor efficiency.

2. EXPERIMENTAL SETUP

A schematic of the main portions of the physical and control system used for this study is provided in Fig. 1. The OP engine was provided by Achates Power Inc. and has the following characteristics.

- Cylinder Count: 1
- Displacement: 1640 [cc]
- Stroke: 108.0 [mm]
- Bore: 98.4 [mm]
- Inlet Port Closing: -129.5 [deg]
- Exhaust Port Opening: 121 [deg]

A gasoline compression ignition strategy using pump gasoline with an 87 anti-knock index was employed for this testing with a split injection strategy consisting of a pilot injection 38 degrees advanced from the main injection. Each crankshaft of the OP engine was coupled to an Avid AF240 axial flux surface mount permanent magnet (SMPM) motor/generator with Semikron SKiiP 1814 GB17E4-3DUW V2 switching units for the inverter. The general operating principle between the OP engine and the electric motors is governed by a torque balance across the mechanical coupling shown in Fig. 1. Neglecting any deflection present in these couplers, the relation for each crankshaft can be expressed as

$$T_{eng}(k) - T_m(k) = I\ddot{\theta}(k) \tag{1}$$

where T_{eng} and T_m denote the torque generated by the engine and the torque of the motor, respectively. The inertia of the rotating mass is I, and $\ddot{\theta}$ denotes the actual rotational acceleration. The motor torque is considered the control input to the system and provides a means of regulating the position, θ, of each engine crankshaft. The desired motor torque required to track a crankshaft position and velocity reference is developed by the position regulator, detailed by Drallmeier et al. (2021a) using measured values of crankshaft position and velocity, as well as cylinder pressure. A field-oriented control scheme is used to regulate the true motor torque (Yusivar et al. (2014)). Both of these controllers, as well as the trajectory optimization scheme outlined in detail in the following sections, are implemented on a dSPACE Microlabbox.

3. TRAJECTORY OPTIMIZATION PROBLEM

Iterative learning control (ILC) is a well documented strategy to improve the performance of repetitive systems (Bristow et al. (2006)). Generally, ILC is used in applications to reduce the tracking error where the ideal tracking reference is known a-priori. However, this work, similar to Cobb et al. (2020), presents a unique view of a repetitive system in which it is of interest to improve an economic performance index through manipulation of

the *tracking reference* rather than reducing the tracking error through manipulation of the *control input*. The ITO methodology detailed in Drallmeier et al. (2022) is used here as it enables constraints to be integrated into the optimization process. For the case of a hybrid opposed piston engine, this is used to maintain the desired phasing between crankshafts as there is no longer a geartrain to couple the piston motion. This trajectory optimization process is formulated as the quadratic programming (QP) problem

$$\begin{aligned} \min_{\Gamma} \quad & J = \frac{1}{2}\Gamma_j^T \Omega_j \Gamma_j + \Psi_j \Gamma_j + c_j \\ s.t. \quad & A\Gamma_j - b = 0 \end{aligned} \tag{2}$$

where the matrix A and vector b are used to define the optimization constraints. The next cycle tracking reference, $r_{j+1}(k)$, which is parameterized using the Fourier series, is updated as

$$r_{j+1}(k) = h(k)^T \Gamma_j. \tag{3}$$

with the subscript j denoting the cycle index and k denoting the time index. The optimization variable $\Gamma_j$is a vector containing the scalar coefficients for the Fourier series, and the vector $h(k)$ contains the trigonometric functions defining the Fourier series. The weighting matrices Ω_j and Ψ_j are defined as

$$\begin{aligned} \Omega_j = 2\sum_{k=1}^{N} \beta_{q0,j}(k)h(k)h(k)^T + \beta_{q1,j}(k)\dot{h}(k)\dot{h}(k)^T + \\ ...+\beta_{qp,j}(k)h^{(p)}(k)h^{(p)}(k)^T \end{aligned} \tag{4}$$

$$\begin{aligned} \Psi_j = \sum_{k=1}^{N} \beta_{l0,j}(k)h(k)^T + \beta_{l1,j}(k)\dot{h}(k)^T + \\ ... + \beta_{lp,j}(k)h^{(p)}(k)^T \end{aligned} \tag{5}$$

where p denotes higher order derivatives of $h(k)$. The value N denotes the number of samples in a period of the repetitive process, which in this case is one revolution of the crankshafts as the OP engine operates on a two stroke cycle. The β variables used to define Ω_j and Ψ_j are derived from the application specific cost function to be minimized. To utilize this ITO method, both (4) and (5) are summed in the time domain over a single learning cycle. Then (2) is solved once after each learning cycle using the results of (4) and (5). As (2) is an equality constrained QP problem, it is solved as a linear system of equations (Nocedal and Wright (2006)). The following sections detail the optimization problem derivation necessary to implement this online trajectory optimization and provide explicit definitions for $h(k)$ and all β values. Note, however, the derivation of this ITO problem will be completed with respect to a single crankshaft as the problem objective and dynamics for each crankshaft are identical. Then, as the ECL must be constrained, the final form of the optimization problem will be given with respect to both the intake and exhaust crankshafts.

3.1 Path Parameterization

With the trajectory of the system, rather than the control input, used as the optimization variable, it is necessary to parameterize the the trajectory variable. This variable is defined as $\theta_d(k)$, the desired position of the crankshaft, and replaces $r_{j+1}(k)$ in (3). Rather than directly optimizing $\theta_d(k)$ for all discrete points $k = 1, 2, \ldots, N$ in a cycle, parameterization reduces the design space and optimization terms for this problem, creating a tractable problem for online implementation. The Fourier series was selected to parameterize $\theta_d(k)$ due to its innate ability to approximate periodic functions. Further, as the Fourier series is made up of infinitely differentiable trigonometric functions, $\theta(k)$ and all of its higher order derivatives can be defined using the same basis parameters, increasing the cost function design space without increasing the number of optimization variables. However, it should be noted that any type of parameterization restricts the form of the path and may result in a sub-optimal reference.

The highest order derivative of the trajectory variable, in this case $\ddot{\theta}_d$, is defined using the Fourier series and the lower order terms $\dot{\theta}_d$ and θ_d are defined through integration, where

$$\ddot{\theta}_d(k) = \ddot{h}(k)^T \Gamma \tag{6a}$$

$$\dot{\theta}_d(k) = \dot{h}(k)^T \Gamma + \omega_{set} \tag{6b}$$

$$\theta_d(k) = h(k)^T \Gamma + \omega_{set} k + \sum_{n=1}^{m} \frac{\gamma_{n,1}}{(n w_{set})^2} - \pi \tag{6c}$$

with $\ddot{h}(k)$ and the basis parameters Γ given as

$$\begin{aligned} \ddot{h}(k) = [1 \;\; \cos(wk) \;\; \sin(wk) \;\; \cos(2wk) \;\; \sin(2wk) \\ \ldots \;\; \cos(m*wk) \;\; \sin(m*wk)]^T \end{aligned} \tag{7}$$

$$\Gamma = [\gamma_0 \;\; \gamma_{1,1} \;\; \gamma_{1,2} \;\; \gamma_{2,1} \;\; \gamma_{2,2} \;\; \cdots \;\; \gamma_{m,1} \;\; \gamma_{m,2}]^T. \tag{8}$$

The form of $\dot{h}(k)$ and $h(k)$ follow directly from integration of (7). In (6b), the constant of integration is w_{set} which denotes the desired velocity setpoint. Similarly, in (6c), the summation of the Γ terms corresponding to cosine terms in $h(k)$ ensures the position at k=0 is $-\pi$ radians, meaning the piston is at bottom dead center (BDC). If a nonzero ECL is desired, the value can then become $-(\pi + ECL)$ for the intake crankshaft, ensuring the intake reference trails the exhaust reference by the desired ECL. In (7), $w = 2\pi f \Delta t$ where f is the frequency of the periodic function and Δt is the sampling period. The number of frequencies contained in the Fourier series parameterization is denoted by m and the number of basis parameters is equal to $2m + 1$. This tunable parameter m presents a trade-off between the computational burden and precision of the path parameterization which will be discussed further in the results section.

3.2 Cost Function Derivation

The objective of this optimization process to maximize the system efficiency. This can be approximated by minimizing any losses from the electric motors as they absorb the torque generated by the engine, assuming a fixed fueling input. While this neglects any possible indicated efficiency improvements for the engine, it was shown in Drallmeier et al. (2021b) that the motor efficiency is the dominant term for intra-cycle efficiency. This leaves the thermal efficiency to be improved through inter-cycle operation, which is outside the scope of this work. Therefore, this problem, for each crankshaft independently, can be stated mathematically as

$$\min_{\Gamma} J = \sum_{k=1}^{N} P_{loss,j}(k) \tag{9}$$

To transcribe this optimization problem into the form provided in (2), the power loss term, P_{loss}, needs to be expressed in terms of the basis parameters Γ. As this term represents instantaneous power lost through the electric motors when extracting work from the crankshaft, it is defined as

$$P_{loss,j}(k) = \frac{3}{2} i_j(k)^2 R + C(\dot{\theta}_{d,j}(k) - e_j(k))^2 \tag{10}$$

which accounts for the resistive and frictional losses of the electric motor. The winding resistance is denoted as R and the coefficient C is used to scale the friction losses by the true rotational velocity where $\dot{\theta}_j(k) = \dot{\theta}_{d,j}(k) - e_j(k)$ with $e_j(k)$ representing velocity tracking error. The quadrature current, $i(k)$, of the electric motors is proportional to the torque generated through the relationship

$$i_j(k) = \frac{T_{m,j}(k)}{9\lambda_m} \tag{11}$$

where λ_m represents the flux-linkage of the motor windings due to the permanent magnets and iron in the motors. For the specific electric motors, the values of $R = 23.3 * 10^{-3}$ Ω, $C = 0.038$ and $\lambda_m = 0.137$ Nm/A are used. Now, we can use (10) and (11) to write the power loss function in terms of $T_m(k)$ and $\dot{\theta}_d(k)$. However, $T_m(k)$ is the control input to the system, obtained from feedback control which is a function of the crankshaft motion (Drallmeier et al. (2021a)). Therefore, the lower level control law for tracking the desired reference, defined by the expression

$$T_{m,j}(k) = \hat{T}_{eng,j}(k) - I\ddot{\theta}_{d,j}(k) + K_{e,j} \tag{12}$$

can be used to replace $T_m(k)$ as a function of $\ddot{\theta}_d(k)$. The value $\hat{T}_{eng}(k) - J\ddot{\theta}_d(k)$ represents the feedforward term based on an approximation of engine torque and the desired crankshaft acceleration while K_e represents the error feedback value accounting for any errors in the torque estimation. Now, changes in $\theta_d(k)$ can be used to manipulate the required $T_m(k)$ for control and improve the work extraction efficiency, resulting in a power loss function of

$$\begin{aligned} P_{loss,j}(k) = &\frac{R(\hat{T}_{eng,j}(k) - J\ddot{\theta}_{d,j}(k) + K_{e,j})^2}{54\lambda^2} \\ &+ C(\dot{\theta}_{d,j}(k) - e_{v,j})^2. \end{aligned} \tag{13}$$

Substituting in the trajectory parameterization defined in (6) and expanding the squared terms in the (13), the cost function in terms of Γ can be defined as

$$\begin{aligned} J = \sum_{k=1}^{N} \Big(&\beta_{q2} \Gamma_j^T \ddot{h}(k) \ddot{h}(k)^T \Gamma_j + \beta_{q1} \Gamma_j^T \dot{h}(k) \dot{h}(k)^T \Gamma_j \\ &+ \beta_{l2,j} \Gamma_j^T \ddot{h}(k) + \beta_{l1,j} \Gamma_j^T \dot{h}(k) + c_j \Big) \end{aligned} \tag{14}$$

where the β coefficients are defined as

$$\beta_{q2} = \frac{RI^2}{54\lambda^2} \tag{15a}$$

$$\beta_{q1} = C \tag{15b}$$

$$\beta_{l2,j} = -\frac{2IR}{54\lambda^2}(\hat{T}_{eng,j} + K_{e,j}) \tag{15c}$$

$$\beta_{l1,j} = 2C(\omega_{set} - e_{v,j}) \tag{15d}$$

$$\tag{15e}$$

and the term c, although independent of Γ and not influential on the optimization, is included here for completeness as

$$\begin{aligned} c_j = &\frac{R}{54\lambda^2} \left(T_{eng,j}^2 + K_{e,j}^2 + 2T_{eng,j} K_{e,j} \right) \\ &+ C \left(\omega_{set}^2 + e_{v,j}^2 - 2e_{v,j}\omega_{set} \right). \end{aligned} \tag{16}$$

Note, for the β coefficients scaling the quadratic Γ terms, the cycle index dependence can be dropped as these coefficients are constant. Further, as the basis parameters Γ are time invariant during a cycle, they can be moved outside of the summation term in (14), thus recovering the form provided in (2).

3.3 ECL Constraint

The previous section provides the parameterized cost function for a single independent motor/crankshaft coupling. However, if the relative motion between the two crankshafts in this hybrid OP engine design is to be constrained, the power loss term should be duplicated for the second crankshaft, which is trivial as the dynamics are identical. This results in a cost function

$$\min_{\Gamma} J = \sum_{k=1}^{N} \left(P_{loss,j}^{exh}(k) + P_{loss,j}^{int}(k) \right) \tag{17}$$

where the superscripts denote the exhaust and intake crankshafts and each term can be expressed in terms of Γ using (14) and (15). However, each crankshaft will use independent Γ parameters as each motion profile can be unique, increasing the number of basis parameters now to $q = 4m + 2$.

With each crankshaft included in the optimization problem, the ECL reference can be fixed at certain points during the cycle using the parameterized form of $\theta_d^{exh}(k) - \theta_d^{int}(k) = ECL$ to populate $A \in \mathbb{R}^{g \times q}$ and $b \in \mathbb{R}^g$ defined in (2) where q is the number of parameters and g is the number of constraints. Intake and exhaust port closing was selected as the point to constrain the ECL as this point in the cycle is highly influential on the breathing dynamics while also determining the trapped volume and thus the effective compression ratio of the engine. Additional points could be selected if necessary, but optimization results show little fluctuation elsewhere in the cycle. Additionally, to ensure a constant average velocity during steady state operation, the value of γ_0 for both the intake and exhaust crankshafts is constrained to 0, which sets the total acceleration of a cycle to 0.

4. RESULTS AND DISCUSSION

This trajectory learning method was tested experimentally under both motored and fired conditions at a speed setpoint of 1600 RPM. For steady state operation, the learning algorithm was triggered once every 30 cycles to reduce the computational load on the dSPACE Microlabbox and allow any tracking error to reach a steady state point before triggering an additional learning cycle. The sampling rate used for collecting measurements for (4) and (5) is 5 kHz. For the motored test, an ECL of 4 degrees was maintained to demonstrate the ability to learn with a nonzero ECL present. A value of $m = 6$ is used for this test. During the fired tests, engine out power was held constant at 35 kW and the ECL was set to 0 degrees. Results quantifying the ITO performance are provided from averaged results of 950 cycles. Note that a

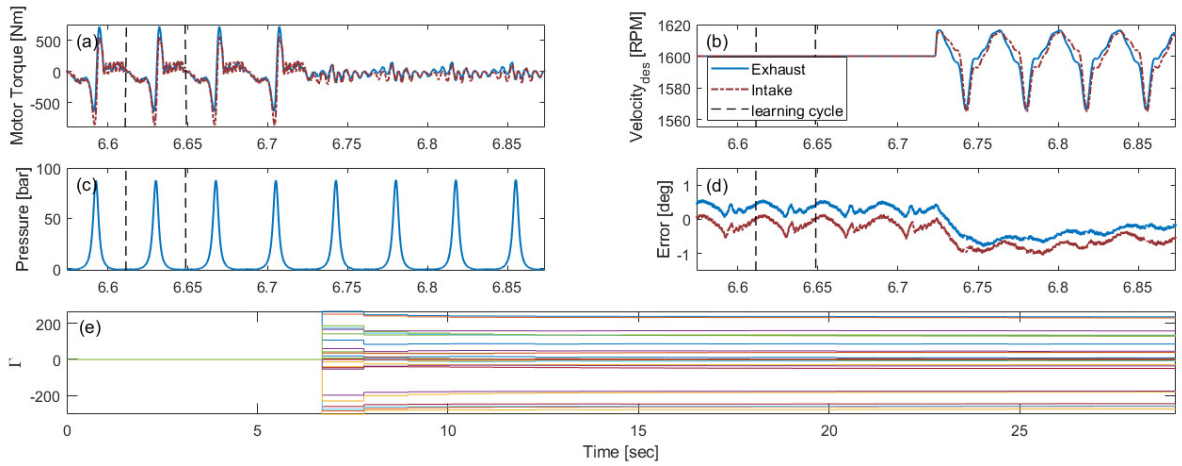

Fig. 2. Results detailing the transition to a learned motion profile at a 4 degree ECL. (a) Motor control torque used to track desired trajectory. (b) Velocity reference. (c) Cylinder pressure. (d) Tracking error of crankshaft. (e) Evolution of the basis parameters during larger timescale to show the rapid convergence of parameters.

positive motor torque denotes work being extracted from the engine, and a negative torque denotes work being put into the engine.

4.1 Motored Conditions

The results in Fig. 2 showing the transition from a constant velocity crankshaft motion reference to a motion reference learned using the ITO method for a motored case. The vertical dashed lines identify the cycle over which (4) and (5) were calculated. The next cycles are then used to calculate Γ_j and then near the 6.72 second mark, the new reference trajectory is introduced at BDC of the exhaust crankshaft. From Fig. 2a it is apparent the learned trajectory provides a drastic reduction in the motor torque required for tracking control of the crankshaft motion while still maintaining an acceptable level of tracking error of less than ± 1 degree for crankshaft position, shown in Fig. 2d. This substantiates the conclusions made in Drallmeier et al. (2021b) that a near constant motor torque profile maximizes the work extraction efficiency. The new crankshaft velocity reference, provided in Fig. 2b, shows the optimal velocity reference fluctuates nearly opposite that of cylinder pressure, shown in Fig. 2c, with a slight difference between the intake and exhaust crankshaft as each will experience a different engine torque due to the ECL. For a constant velocity reference, the motor is required to supply increasing torque to the crankshaft as cylinder pressure increases, only extracting work as each crankshaft passes top dead center (TDC). Rather, the learned trajectory allows the crankshaft to slow during compression and accelerate during expansion, smoothing out the motoring torque required to maintain an average cycle velocity. Further, as the ECL is maintained with the learned trajectory, there is negligible impact to the cylinder pressure after enabling learning.

The basis parameters, Γ, are shown in Fig. 2e over the full recording length rather than only the cycles where learning was enabled. As the quadratic β coefficients in (15a) and (15b) are positive and the number of samples for each cycle is larger than the number of basis parameters used, the optimization problem given by (2) is guaranteed

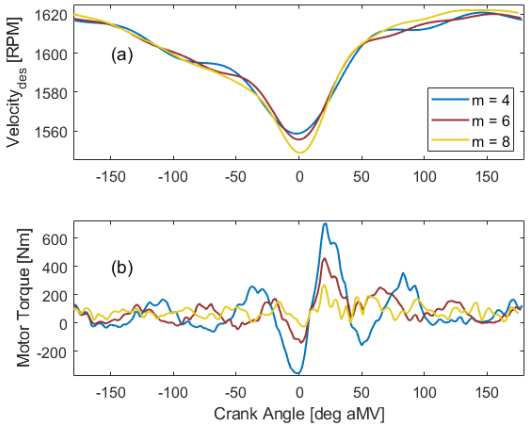

Fig. 3. Single cycle results for the exhaust crankshaft of the (a) learned velocity reference and (b) required motor torque input for tracking the reference for fired cases at 1600 RPM and 35kW engine out power.

to be strictly convex (see Proposition 1 in Drallmeier et al. (2022)). As such, the first values obtained for the Γ parameters are near the optimal location. However, as (15c) and (15d) are time varying and dependent on measured values, a few learning iterations are required before Γ reaches steady state.

4.2 Fired Conditions

The ITO method can also be utilized during fired engine cycles to improve system efficiency while extracting positive work from the engine. Figure. 3 provides a single cycle comparison of ITO method results under fired conditions with increasing values of m which denotes the number of frequencies contained in the Fourier series parameterization. This figure only shows the exhaust crankshaft results as each crankshaft operates similarly for the 0 ECL setpoint. A constant velocity baseline cannot be utilized here as the engine torque which the motor would have to match exceeds the capabilities of the electric motors. As m is increased, the trajectory can better approximate the ideal reference and a significant reduction in the peak-to-

Table 1. Cycle average results for the fired cases over 950 cycles.

	m = 4	m = 6	m = 8
Motor Torque Amplitude [Nm]	1072.8	613.8	297.1
Electric Machine η [%]	72.3	78.0	81.4

peak motor torque is achieved. The mean value of peak-to-peak torque amplitude from 950 engine cycles for each case is quantified in Tab. 1.

An additional performance index to quantify these results is the electric machine efficiency, and indeed from $m = 4$ to $m = 8$, there is an increase in efficiency of 9.1% for the mechanical to electrical conversion of power through the electric machines, including the inverter losses, as shown in Tab.1. Further improvement beyond m=8 is limited due to the quadratic computational complexity associated with the matrix multiplication required in (4) and (5) which must be calculated at each sample point for the summation. However, it should be noted that this quantification of efficiency here underestimates the improvements capable for this system as the current motors are extremely oversized for the application. They were sized for peak torque rather than nominal power ratings with each AVID AF240 rated for a nominal power of 188 kW. The engine in this case is operating at a 35 kW setpoint, meaning each crankshaft is producing approximately 17.5 kW.

5. CONCLUSION

This paper presents an application of the ITO method for learning the optimal crankshaft motion profile of a hybrid opposed piston engine. The ITO method can be implemented with little prior knowledge of the system and reduces the need for offline optimization and the impact of model uncertainty on online performance. The effectiveness of the learning algorithm is dependent largely on the precision of the trajectory parameterization which is limited by the computational time allowed by the physical system.

ACKNOWLEDGEMENTS

The authors would like to acknowledge members of Achates Power, Inc, specifically Ashwin Salvi and Ming Huo, for their intellectual support as well as financial support from the Automotive Research Center (ARC) in accordance with Cooperative Agreement W56HZV-19-2-0001 U.S. Army DEVCOM GVSC.

REFERENCES

Bristow, D.A., Tharayil, M., and Alleyne, A.G. (2006). A survey of iterative learning control. *IEEE Control Systems*, 26(3), 96–114. doi:10.1109/mcs.2006.1636313.

Cobb, M.K., Barton, K., Fathy, H., and Vermillion, C. (2020). Iterative learning-based path optimization for repetitive path planning, with application to 3-d crosswind flight of airborne wind energy systems. *IEEE Trans Contr Syst Technol*, 28(4), 1447–1459. doi:10.1109/tcst.2019.2912345.

Drallmeier, J., Siegel, J.B., Middleton, R., Stefanopoulou, A.G., Salvi, A., and Huo, M. (2021a). Modeling and control of a hybrid opposed piston engine. In *ASME 2021 ICEF*. American Society of Mechanical Engineers. doi:10.1115/icef2021-67541.

Drallmeier, J.A., Siegel, J.B., and Stefanopoulou, A.G. (2022). Iterative learning-based trajectory optimization using fourier series basis functions. *IEEE Control Systems Letters*, 6, 2180–2185. doi:10.1109/lcsys.2021.3139986.

Drallmeier, J.A., Hofmann, H., Middleton, R., Siegel, J., Stefanopoulou, A., and Salvi, A. (2021b). Work extraction efficiency in a series hybrid opposed piston engine. In *SAE Technical Paper Series*. SAE International. doi:10.4271/2021-01-1242.

Enang, W. and Bannister, C. (2017). Modelling and control of hybrid electric vehicles (a comprehensive review). *Renewable Sustainable Energy Rev.*, 74, 1210–1239. doi:10.1016/j.rser.2017.01.075.

Herold, R.E., Wahl, M.H., Regner, G., Lemke, J.U., and Foster, D.E. (2011). Thermodynamic benefits of opposed-piston two-stroke engines. In *SAE Technical Paper Series*. SAE International. doi:10.4271/2011-01-2216.

Naik, S., Johnson, D., Koszewnik, J., Fromm, L., Redon, F., Regner, G., and Fuqua, K. (2013). Practical applications of opposed-piston engine technology to reduce fuel consumption and emissions. In *SAE Technical Paper Series*. SAE International. doi:10.4271/2013-01-2754.

Nocedal, J. and Wright, S. (2006). *Numerical Optimization*. Springer.

Payri, F., Lopez, J.J., Pla, B., and Bustamante, D.G. (2014). Assessing the limits of downsizing in diesel engines. In *SAE Technical Paper Series*. SAE International. doi:10.4271/2014-32-0128.

Pirault (2010). *Opposed piston engines : evolution, use, and future applications*. SAE International, Warrendale, Pa.

Serrano, J.R., García, A., Monsalve-Serrano, J., and Martínez-Boggio, S. (2021). High efficiency two stroke opposed piston engine for plug-in hybrid electric vehicle applications: Evaluation under homologation and real driving conditions. *Appl Energ*, 282, 116078. doi:10.1016/j.apenergy.2020.116078.

Willcox, M.A., Cleeves, J.M., Jackson, S., Hawkes, M., and Raimond, J. (2012). Indicated cycle efficiency improvements of a 4-stroke, high compression ratio, s.i., opposed-piston, sleeve-valve engine using highly delayed spark timing for knock mitigation. In *SAE Technical Paper Series*. SAE International. doi:10.4271/2012-01-0378.

Young, A.G., Costall, A.W., Coren, D., and Turner, J.W.G. (2021). The effect of crankshaft phasing and port timing asymmetry on opposed-piston engine thermal efficiency. *Energies*, 14(20), 6696. doi:10.3390/en14206696.

Yusivar, F., Hidayat, N., Gunawan, R., and Halim, A. (2014). Implementation of field oriented control for permanent magnet synchronous motor. In *2014 International Conference on Electrical Engineering and Computer Science (ICEECS)*. IEEE. doi:10.1109/iceecs.2014.7045278.